Available online at www.sciencedirect.com
SCIENCE DIRECT®
Journal of Colloid and Interface Science 273 (2004) 218–223
JOURNAL OF Colloid and Interface Science
www.elsevier.com/locate/jcis

Electrical potential in a cylindrical double layer: a functional theory approach

Shiojenn Tseng,[a,*] Ji-Ming Jiang,[b] and Jyh-Ping Hsu [b]

[a] *Department of Mathematics, Tamkang University, Tamsui, Taipei 25137, Taiwan, Republic of China*
[b] *Department of Chemical Engineering, National Taiwan University, Taipei 10617, Taiwan, Republic of China*

Received 9 July 2003; accepted 25 September 2003

Abstract

Employing an iterative method in functional theory, the electrical potential distribution for the case of a cylindrical surface is solved. Although the analytical result derived is of an iterative nature, the second-order solution is found to be sufficiently accurate under conditions of practical significance. For the case of constant surface potential, the radius and the surface potential of a cylindrical surface can be estimated based on the extreme of the electrical potential distribution. The effects of the key parameters, including the number and the valence of the ions on a surface, the length of a particle, the relative permittivity of the liquid phase, the temperature, and the concentration of electrolyte on the surface potential, are examined. The general behavior of these effects is similar to that for a spherical surface, except that the surface potential of a cylindrical surface is independent of the electrolyte concentration. The present approach is also applicable to the case where a cylindrical surface remains at a constant charge density.

Keywords: Electrical potential; Cylindrical surface; Poisson–Boltzmann equation; Functional theory

1. Introduction

The spatial variation of the electrical potential for a charged surface in an electrolyte solution can be described by a Poisson–Boltzmann equation [1,2], a nonlinear partial differential equation. Although this equation is of an approximate nature, its performance is found to be satisfactory for symmetric, univalent electrolytes at concentrations of practical significance [3]. In spite of its simple mathematical form, the only exactly analytically solvable Poisson–Boltzmann equation is that for an infinite planar surface in a symmetric electrolyte solution. Other than this case, it can be solved only numerically or approximately only. For instance, under the Debye–Hückel condition, that is, sufficiently low electrical potential, a Poisson–Boltzmann equation can be approximated by a linearized equation, which can then be solved analytically for simple geometries and boundary conditions [1,2]. Seeking the solution of a Poisson–Boltzmann equation is of fundamental significance in colloid and interface science. The evaluation of the stability behavior of a dispersion, the calculation of the rate of adsorption of entities to a surface, and the description of electrokinetic phenomena such as electrophoresis, to name a few examples, all involve this procedure. Apparently, to establish a systematic approach to the resolution of a Poisson–Boltzmann equation is highly desirable. One possible approach is that based on the functional theory. It was pointed out that the Poisson–Boltzmann equation for a symmetric electrolyte could be solved with the iterative method in the functional theory for an arbitrary level of electrical potential [4–6]. Wang et al. [7], for example, adopted this approach to solve the Poisson–Boltzmann equation for a spherical surface. They claimed that this approach is superior to the conventional methods because it is applicable to a general electrical potential level and is capable of providing information about the radius and the surface potential of a spherical colloidal particle [8,9].

In this study, the analysis of Wang et al. [8,9] is extended to a cylindrical surface. An attempt is made to derive an analytical, iterative solution, which is sufficiently accurate for the description of the electrical potential distribution in a cylindrical double layer. Also, the influence of the physi-

* Corresponding author.
E-mail address: tseng@math.tku.edu.tw (S. Tseng).

0021-9797/$ – see front matter
doi:10.1016/j.jcis.2003.09.029

cal properties of a cylindrical particle and those of the liquid phase on the surface potential of a particle is discussed.

2. Analysis

The electrical potential $\psi(r)$ in the diffuse double layer near a charged surface can be described by the Poisson–Boltzmann equation [1,2],

$$\nabla^2\psi(r) = -\frac{\rho(r)}{\varepsilon}, \tag{1}$$

where ∇^2, ρ, and ε denote, respectively, the Laplace operator, the space charge density, and the relative permittivity of the medium. Let us consider the electrical potential outside a nonconductive, infinitely long cylinder of radius R immersed in an electrolyte solution. In this case, Eq. (1) becomes

$$\frac{1}{r}\frac{d}{dr}\left(r\frac{d\psi}{dr}\right) = -\frac{\rho(r)}{\varepsilon}, \quad R < r. \tag{2}$$

The boundary conditions associated with this equation are assumed to be

$$\psi \to 0, \quad R \ll r, \tag{3a}$$

$$\psi = \psi(R), \quad r = R, \tag{3b}$$

where $\psi(R)$ is the surface potential. For the case of a z:z electrolyte with a number concentration n_0, Eq. (2) becomes

$$\nabla^2\psi(r) = -\frac{2zen_0}{\varepsilon}\sinh\left(-\frac{ze\psi}{k_BT}\right), \quad R < r. \tag{4}$$

Under the Debye–Hückel condition, the solution to this equation subject to Eq. (3a) is

$$\psi(r) = AK_0(\kappa r), \quad R < r, \tag{5}$$

where A is a constant, K_0 is the zeroth order Bessel function of the second kind, and $\kappa = (2000e^2N_Acz^2/\varepsilon k_BT)^{1/2}$ is the reciprocal Debye length, e, N_A, c, z, k_B, and T being, respectively, the elementary charge, Avogadro's number, the molar bulk ion concentration, the valence of bulk ions, the Boltzmann constant, and the absolute temperature. Applying Eq. (3b) to Eq. (5) gives

$$\psi(r) = \psi(R)\frac{K_0(\kappa r)}{K_0(\kappa R)}, \quad R < r, \tag{6}$$

where R and $\psi(R)$ can be determined experimentally. Alternatively, if the cylindrical particle is infinitely thin and the electrolyte solution is infinitely dilute, then it can be shown that Eq. (5) yields (Appendix A)

$$\psi(r) = \frac{2\sigma}{\varepsilon}K_0(\kappa r), \tag{7}$$

where σ is the linear charge density (C/m) of the particle. While the exact analytical solution to Eq. (4) under general conditions cannot be derived at the present stage, an iterative solution based on the functional theory and Eq. (7) can be obtained.

Let us consider a set C, which comprises the functions $(\psi, \phi, \ldots)$. These functions are continuous, and have at least second-order derivatives in an open interval (a, b), where a and b are two different real numbers. The maximum norm of a function ψ is defined as [5,6]

$$\|\psi\| = \max_{a<r<b}\left|\psi(r)\right|. \tag{8}$$

It can be shown that, for any two functions ψ and ϕ in C and λ a real number,

$$\|\psi\| \geqslant 0, \tag{9a}$$

$$\|\psi\| + \|\phi\| \geqslant \|\psi + \phi\|, \tag{9b}$$

$$\|\lambda\psi\| = |\lambda|\|\psi\|. \tag{9c}$$

According to the functional theory, the set C forms a Banach space B. We consider the operator $\hat{P}$, which has the property

$$\psi = \hat{P}\psi, \quad \psi \in B. \tag{10}$$

Also, if $\hat{P}$ satisfies the Lipschitz condition, then

$$\left\|\hat{P}\psi - \hat{P}\phi\right\| \leqslant \alpha\|\psi - \phi\|, \quad \psi, \phi \in B, \tag{11}$$

where α is the Lipschitz constant ($0 \leqslant \alpha < 1$). Then, beginning with an arbitrary function $\psi_0 \in B$, we have [5]

$$\psi_{n+1} = \hat{P}\psi_n, \quad n = 0, 1, 2, \ldots \tag{12}$$

and

$$\lim_{n\to\infty}\psi_n(r) = \psi(r). \tag{13}$$

Here, $\psi_n(r)$ is the nth-order iterative approximate solution of Eq. (12), and $\psi(r)$ is the exact solution of the equation

$$\psi(r) = \hat{P}\psi(r). \tag{14}$$

As will be illustrated latter, this approach is applicable to the case of cylindrical coordinates. If Eq. (4) is expressed in the form of Eq. (10), then $\hat{P}$ can be constructed as

$$\begin{aligned}\hat{P} &= \frac{k_BT}{ze}\sinh^{-1}\left[\frac{\varepsilon}{2n_0ze}\nabla_r^2\right] \\ &= \frac{k_BT}{ze}\sinh^{-1}\left[\frac{ze}{k_BT\kappa^2}\nabla_r^2\right].\end{aligned} \tag{15}$$

It can be also shown [8] that

$$\begin{aligned}\hat{P}\psi &= \frac{k_BT}{ze}\sinh^{-1}\left[\frac{ze}{k_BT\kappa^2}\nabla_r^2\right]\psi \\ &= \frac{k_BT}{ze}\sinh^{-1}\left[\frac{ze}{k_BT\kappa^2}\nabla_r^2\psi\right].\end{aligned} \tag{16}$$

Here, Eq. (7) is adopted as the initial or zeroth-order iterative solution $\psi_0(r)$, and the higher-order iterative solutions, $\psi_n(r)$, $n = 1, 2, \ldots$, are generated by Eqs. (12) and (16).

Among these, the first three iterative solutions are, respectively,

$$\psi_1(r) = \hat{P}\psi_0(r) = \frac{k_BT}{ze}\sinh^{-1}\left[\frac{ze}{k_BT}\psi_0(r)\right] = \frac{k_BT}{ze}\sinh^{-1} f, \tag{17}$$

$$\psi_2(r) = \hat{P}\psi_1(r) = \frac{k_BT}{ze}\sinh^{-1}\left\{\frac{f}{\sqrt{1+f^2}}\left[1-\frac{1}{1+f^2}\left(\frac{1}{\kappa}\frac{df}{dr}\right)^2\right]\right\}, \tag{18}$$

$$\psi_3(r) = \hat{P}\psi_2(r) = \frac{k_BT}{ze}\sinh^{-1}\left\{\frac{1}{\kappa^2\sqrt{1+g^2}}\left[\frac{2}{r}\frac{dg}{dr}+\frac{d^2g}{dr^2} - \frac{g}{1+g^2}\left(\frac{dg}{dr}\right)^2\right]\right\}, \tag{19}$$

where $f = ze\psi_0/k_BT$,

$$g = \frac{f}{\sqrt{1+f^2}}\left[1-\frac{1}{1+f^2}\left(\frac{1}{\kappa}\frac{df}{dr}\right)^2\right], \tag{19a}$$

$$\frac{dg}{dr} = \frac{(2f^2-1)\left(\frac{df}{dr}\right)^3+(1+f^2)\frac{df}{dr}\left[\kappa^2-2f\frac{d^2f}{dr^2}\right]}{\kappa^2(1+f^2)^{5/2}}, \tag{19b}$$

$$\frac{d^2g}{dr^2} = \left(\left[5(-1+f^2+2f^4)\left(\frac{df}{dr}\right)^2+\kappa^2(1+f^2)^2\right]\frac{d^2f}{dr^2} + (9f-6f^3)\left(\frac{df}{dr}\right)^4 - 3\kappa^2 f(1+f^2)\left(\frac{df}{dr}\right)^2 - 2f(1+f^2)^2\left[\frac{df}{dr}\frac{d^3f}{dr^3}+\left(\frac{d^2f}{dr^2}\right)^2\right]\right) \Big/ \kappa^2(1+f^2)^{7/2}. \tag{19c}$$

It should be indicated that the choice of $\psi_0 \in B$ is arbitrary but the rate of convergence of $\psi_n(r)$ to $\psi(r)$ is highly dependent upon this choice, as will be discussed latter. For a spherical surface, it is known that if $\psi_0(r)$ is properly chosen and $\hat{P}$ is well-constructed, then the second-order iterative solution is sufficiently accurate [9]. Fig. 1 shows the first four iterative solutions, $\psi_0(r)$, $\psi_1(r)$, $\psi_2(r)$, and $\psi_3(r)$. For comparison, the exact numerical solution is also presented in this figure. As can be seen in Fig. 1, the second-order iterative solution $\psi_2(r)$ is also sufficiently accurate for a cylindrical surface. As for the case of a spherical surface, $\psi_n(r)$, $n \geqslant 2$, exhibits a local maximum at R. This nature can be used to judge the radius of a particle [8,9]. Note that the value of $\psi_n(r)$, $n \geqslant 2$, for $r < R$ has mathematical, but no physical meaning. Equation (17) can be rewritten as

$$\sinh\left[\frac{ze}{k_BT}\psi_1(r)\right] = \frac{ze}{k_BT}\psi_0(r). \tag{20}$$

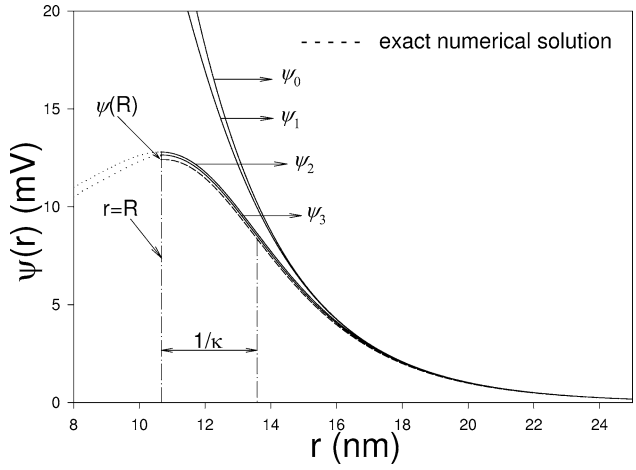

Fig. 1. Variation of electrical potential ψ as a function of the distance from the center of a cylinder r. ψ_0 is the value of ψ under the Debye–Hückel condition. ψ_1, ψ_2, and ψ_3 are the first-, the second-, and the third-order iterative solution, respectively. Parameters used are $Z_p = 1$, $m_a = 100$, $c = 0.01$ M, $T = 298.16$ K, $\varepsilon = 6.954 \times 10^{-10}$ CV^{-1}/m, and $L = 200$ nm. Short dashed curve, the exact numerical result for the case when $R = 10.65$ nm and $\psi(R) = 12.4$ mV.

Under the Debye–Hückel condition, expanding the left-hand side of this expression in Taylor series in terms of $\psi_1(r)$ and retaining the linear term, we obtain

$$\psi_1(r) \cong \psi_0(r). \tag{21}$$

Similarly, it can be shown that under the Debye–Hückel condition, $\psi_n(r) \cong \psi_{n-1}(r)$, which implies that $\psi_n(r) \cong \psi_0(r)$. Fig. 1 also indicates that if r is large, $\psi_0(r)$ is satisfactory, which is expected because ψ is low if r is large, and the Debye–Hückel condition is automatically satisfied. Note that while both ψ_0 and ψ_1 increase rapidly as r decreases, which is certainly unrealistic, ψ_2 approaches $\psi(R)$, the exact numerical solution, as $r \to R$.

In general, the solution of the Poisson–Boltzmann equation based on the Debye–Hückel condition will overestimate the potential near a charged surface. This is illustrated in Fig. 1, where $\psi_2(r) < \psi_1(r) < \psi_0(r)$. Because the operator $\hat{P}$ is constructed based on the Poisson–Boltzmann theory and the Debye–Hückel result $\psi_0(r)$ is the zeroth-order solution, among the approximate solutions, $\psi_1(r)$ and $\psi_2(r)$ must be more accurate than $\psi_0(r)$, and $\psi_2(r)$ more accurate than $\psi_1(r)$, according to the functional theory [6], and this is justified in Fig. 1. In fact, it can be shown that $\psi_{n+1}(r)$ is more accurate than $\psi_n(r)$, $n \geqslant 0$. Note that in the derivation of Eq. (7), a cylindrical particle is treated as a charged line segment in an infinitely dilute electrolyte solution. In this case, since the distance from the center of the particle, r, is much greater than the particle radius, R, the Debye–Hückel condition is satisfied. This explains why all the iterative solutions coincide if r is sufficiently large. On the other hand, if the potential is high or r is small, the solution of the Poisson–Boltzmann equation will deviate from that under the Debye–Hückel condition. Fig. 1 shows that although both ψ_0 and ψ_1 seem to diverge as $r \to R$, ψ_2 and ψ_3 approach a maximum

as $r \to R$. Note that since the interior of a particle is free of charge, $\psi(r)$ should be flat for $r < R$, which is justified by the exact numerical solution presented in Fig. 1. This property can be used to estimate the surface potential $\psi(R)$. To illustrate, $\psi_2(r)$ is regarded as the exact electrical potential; the same arguments are applicable to higher order solutions if they are available. Because the electrical potential is flat for $r < R$, we have

$$\frac{d\psi_2(r)}{dr} = 0, \quad r = R. \tag{22}$$

Substituting Eq. (18) into this expression yields

$$\frac{d\psi_2(r)}{dr} = \mu^2 K_1^2(\kappa r) + \mu^4 K_0^2(\kappa r)\big(K_0^2(\kappa r) - 2K_1^2(\kappa r)\big) + \mu^2 K_0(\kappa r)K_2(\kappa r)\big(1 + \mu^2 K_0^2(\kappa r)\big) - 1 = 0, \tag{23}$$

where $\mu = zeA/k_BT$. This nonlinear algebraic equation needs to be solved numerically. The Newton–Raphson method is found to be effective, using $R = 5/\kappa$ as an initial estimate. Usually, a convergent root can be obtained after a few iterations.

3. Results and discussion

Assume that an ion on the surface of a cylindrical particle carries Z_p elementary charges and the particle comprises m_a ions; then the constant A in Eq. (7) can be expressed as $A = 2\sigma/\varepsilon \cong 2Q/\varepsilon L = 2m_a Z_p e/\varepsilon L$, where Q and L are, respectively, the total amount of charge and the length of the particle. Therefore, Eq. (7) becomes

$$\psi(r) = \frac{2m_a Z_p e}{\varepsilon L} K_0(\kappa r). \tag{24}$$

That is, the surface potential $\psi(R)$ may be dependent upon $Z_p, m_a, c, T, \varepsilon$, and L. Note that, because $\psi(r) = \psi(R)$ for $r \leqslant R$, R can be viewed as the characteristic length in the radial direction at which $\psi(r)$ begins to become flat as r decreases. This idea was proposed by Wang et al. [8,9] for the estimation of the radius of a spherical surface.

The influences of the key parameters of the system under consideration, including the number of ions on a surface m_a, the length of a cylinder L, the relative permittivity of the liquid phase ε, the valence of the ions on a surface Z_p, the absolute temperature T, and the concentration of electrolyte c, on the variation of the surface potential $\psi(R)$ are presented in Fig. 2 through Fig. 7, respectively. Fig. 2 reveals that $\psi(R)$ increases with the increase in m_a, which is expected because the larger the m_a the more the amount of charges on a surface. However, under the conditions assumed, the rate of increase in $\psi(R)$ decreases rapidly when m_a reaches about 200. Similar behavior was also observed by Wang et al. for the case of a spherical surface [9]. Fig. 3 indicates that for a fixed amount of surface charge, $\psi(R)$ decreases with L. This is because the longer the particle, the lower the linear charge density. Note that $\psi(R)$ is nonlinearly dependent on L. As illustrated in Fig. 4 through Fig. 6, $\psi(R)$ decreases with the increase in ε or Z_p, but increases roughly linearly with the increase in T. Similar behavior was also observed for a spherical surface [9]. Fig. 7 reveals that $\psi(R)$ is independent of the electrolyte concentration, which differs from that that observed by Wang et al. [9] for a spherical surface, where the surface potential increases from 5.6 to 8.3 mV as the concentration of electrolyte varies from 10^{-6} to 1 mol/l.

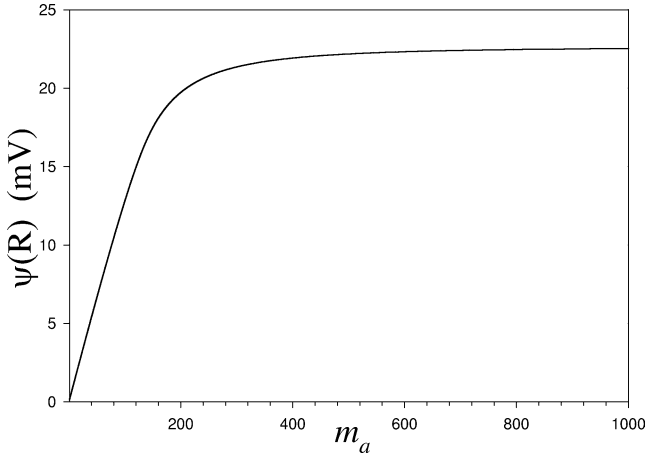

Fig. 2. Variation of surface potential as a function of the number of ions on particle surface for the case when $Z_p = 1$, $c = 0.01$ M, $T = 298.16$ K, $\varepsilon = 6.954 \times 10^{-10}$ CV^{-1}/m, and $L = 200$ nm.

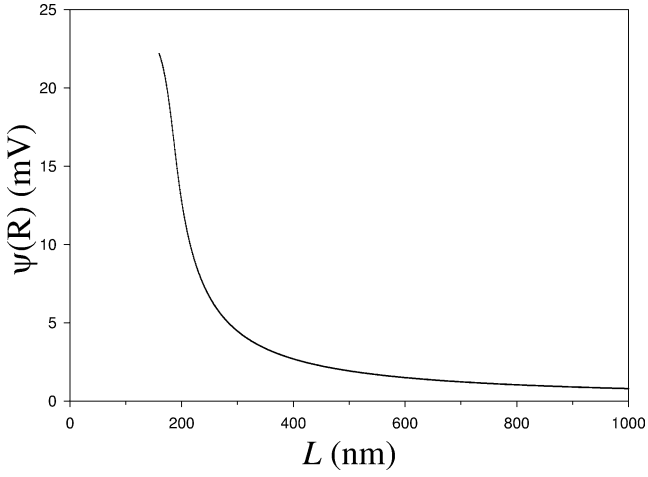

Fig. 3. Variation of surface potential as a function of particle length for the case when $Z_p = 1$, $m_a = 100$, $c = 0.01$ M, $T = 298.16$ K, and $\varepsilon = 6.954 \times 10^{-10}$ CV^{-1}/m.

For the case a surface is remained at constant charge density, the boundary condition expressed in Eq. (3) should be rewritten in terms of the surface charge density σ_S as

$$\sigma_S = -\varepsilon \frac{d\psi}{dr}, \quad r = R. \tag{25}$$

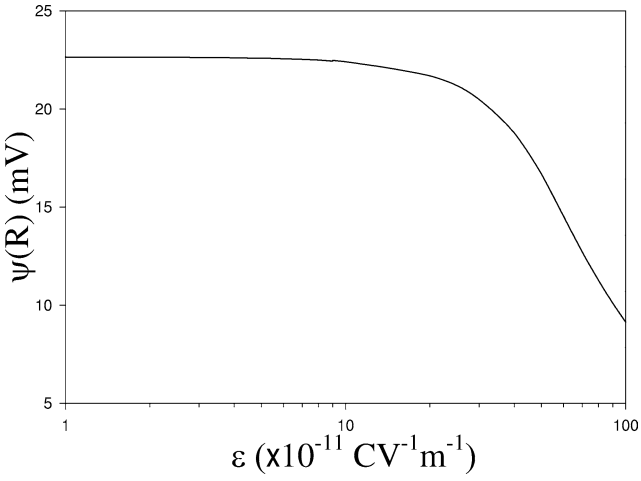

Fig. 4. Variation of surface potential as a function of relative permittivity of the medium for the case when $Z_p = 1$, $m_a = 100$, $c = 0.01$ M, $T = 298.16$ K, and $L = 200$ nm.

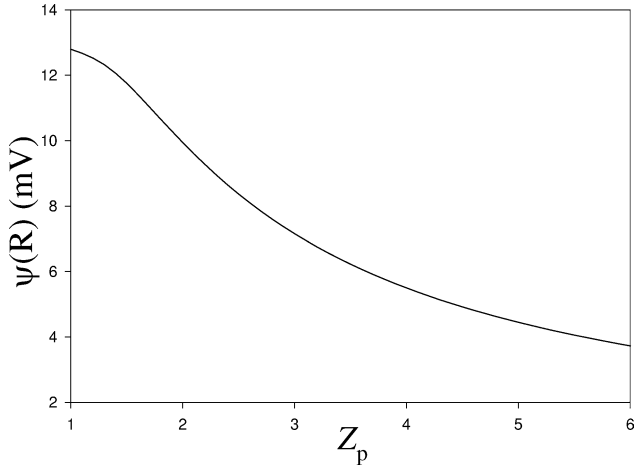

Fig. 5. Variation of surface potential as a function of ionic valence for the case when $m_a = 100$, $c = 0.01$ M, $T = 298.16$ K, $\varepsilon = 6.954 \times 10^{-10}$ $\mathrm{CV}^{-1}/\mathrm{m}$, and $L = 200$ nm.

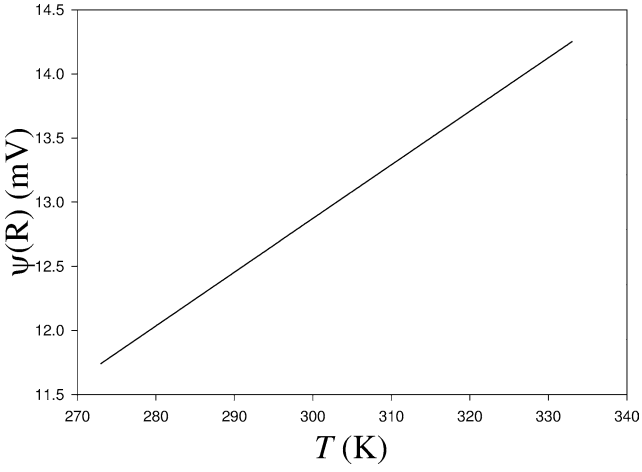

Fig. 6. Variation of surface potential as a function of absolute temperature for the case when $Z_p = 1$, $m_a = 100$, $c = 0.01$ M, $\varepsilon = 6.954 \times 10^{-10}$ $\mathrm{CV}^{-1}/\mathrm{m}$, and $L = 200$ nm.

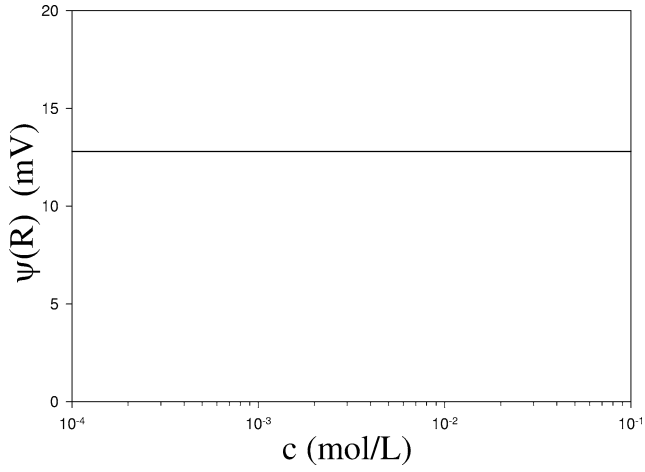

Fig. 7. Variation of surface potential as a function of electrolyte concentration for the case when $Z_p = 1$, $m_a = 100$, $T = 298.16$ K, $\varepsilon = 6.954 \times 10^{-10}$ $\mathrm{CV}^{-1}/\mathrm{m}$, and $L = 200$ nm.

In this case the surface potential can be estimated by seeking the unique positive root of the equation

$$\frac{d\psi_2(r)}{dr} = \mu^2 K_1^2(\kappa r) + \mu^4 K_0^2(\kappa r)\big(K_0^2(\kappa r) - 2K_1^2(\kappa r)\big) + \mu^2 K_0(\kappa r) K_2(\kappa r)\big(1 + \mu^2 K_0^2(\kappa r)\big) - 1 = -\sigma_S/\varepsilon. \tag{26}$$

It can shown that the maximum norms $\|\psi_n - \psi\|$ and $\|\psi_1 - \psi_0\|$ follows the relation [6,10]

$$\|\psi_n - \psi\| \leqslant \frac{\alpha^n}{1-\alpha}\|\psi_1 - \psi_0\|, \tag{27}$$

where the Lipschitz constant can be estimated by $\alpha = \|\psi_2 - \psi_1\|/\|\psi_1 - \psi_0\|$. Therefore, the smaller the value of $\alpha^n/(1-\alpha)$, the more accurate the nth-order solution ψ_n is. Table 1 shows the estimated values of α and $\alpha^n/(1-\alpha)$ at various radii of a particle. This table reveals that both α and $\alpha^n/(1-\alpha)$ are smaller than unity, and $\alpha^n/(1-\alpha)$ decreases with the increase in n. These imply that the operator $\hat{P}$ defined in Eq. (15) satisfies the Lipschitz condition, and ψ_n is convergent as $n \to \infty$. The influence of the choice of the zeroth-order solution, ψ_0, on the rate of convergence is illustrated in Table 2. For illustration, three cases are considered: $\psi_0 = AK_0(\kappa r)$ in case I, $\psi_0 = A[\ln(2/r) - 0.5772](1 + r^2/4)$ in case II, and $\psi_0 = A\ln(2/r)$ in case III. The ψ_0 in case II and that in case III are approximate expressions for $AK_0(\kappa r)$, obtained by expanding it around $r = 0$ and truncating higher-order terms. Table 2 reveals that the rate of convergence of ψ_n follows the order case I > case II > case III.

In summary, the Poisson–Boltzmann equation for the case of a cylindrical surface immersed in a symmetric electrolyte is solved by a functional theory approach for an arbitrary level of electrical potential. Although this approach is of an iterative nature, the second-order solution is found to be sufficiently accurate, and therefore, it provides an efficient way of solving the Poisson–Boltzmann equation in

Table 1
Variation of Lipschitz constant α and relative errors in electrical potential at various particle radius R, which is obtained by varying the number of ions on particle surface m_a

R (nm)	8.50	9.53	10.65
$\|\psi_1(r) - \psi_0(r)\|$ (mV)	84.67	55.36	34.6
$\|\psi_2(r) - \psi_1(r)\|$ (mV)	19.98	16.12	12.80
α	0.236	0.291	0.370
$\alpha/(1-\alpha)$	0.309	0.410	0.587
$\alpha^2/(1-\alpha)$	0.073	0.119	0.217
$\alpha^3/(1-\alpha)$	0.017	0.035	0.080

Key: $Z_p = 1$, $c = 0.01$ M, $T = 298.16$ K, $\varepsilon = 6.954 \times 10^{-10}$ $\mathrm{CV}^{-1}/\mathrm{m}$, and $L = 200$ nm.

Table 2
Variation of Lipschitz constant and relative errors in electrical potential for various choices of ψ_0

ψ_0	$AK_0(\kappa r)$	$A[\ln(2/r) - 0.5772](1 + r^2/4)$	$A\ln(2/r)$
R(nm)	8.50	8.71	9.14
$\|\psi_1(r) - \psi_0(r)\|$ (mV)	84.67	85.99	90.41
$\|\psi_2(r) - \psi_1(r)\|$ (mV)	19.98	21.67	24.50
α	0.236	0.252	0.271
$\alpha/(1-\alpha)$	0.309	0.337	0.371
$\alpha^2/(1-\alpha)$	0.073	0.085	0.101
$\alpha^3/(1-\alpha)$	0.017	0.021	0.027

Key: same as in Table 1.

cylindrical coordinates. Unlike the conventional approach, where a differential equation is solved subject to specified boundary conditions, the present approach allows estimating both the surface potential and the radius of a cylindrical particle. That is, the physical properties of a particle can be deduced from the solution of the corresponding Poisson–Boltzmann equation. The present iterative solution is of uniform convergence nature; that is, the higher the order of a solution the more accurate it is. The other iterative approaches do not (or cannot be proven to) have this nice property. In addition, the other iterative approaches usually use the curvature of a surface or the thickness of a double layer as perturbed parameter; thereby their rate of convergence depends on the physical properties of a system, which is not the case for the present approach.

Acknowledgment

This work is supported by the National Science Council of the Republic of China.

Appendix A

According to Gauss's law,

$$\int_S \mathbf{E} \cdot d\Omega = \frac{Q_{\text{enclosed}}}{\varepsilon}, \tag{A.1}$$

where $\mathbf{E}$ and Q_{enclosed} are, respectively, the electric field and the charge in a volume enclosed by surface S. Suppose that the radius of the cylindrical particle is infinitely small and the electrolyte solution is infinitely dilute. Then Eqs. (5) and (A.1) yield

$$A = \frac{2Q}{\varepsilon L}, \tag{A.2}$$

where L and Q are, respectively, the length of the particle and the total amount of charge on its surface. Here, the relation

$$\lim_{r\to 0}\left[rK_1(\kappa r)\right] = 1/\kappa \tag{A.3}$$

is applied. Defining the linear charge density $\sigma = Q/L$, Eq. (7) in the text can be recovered.

References

[1] R.J. Hunter, Foundations of Colloid Science, vol. 1, Oxford Univ. Press, London, 1989.
[2] P.C. Hiemenz, Principles of Colloid and Surface Chemistry, Dekker, New York, 1977.
[3] S.L. Carnie, G.M. Torrie, Adv. Chem. Phys. 56 (1984) 141.
[4] B. Beauzamy, Introduction to Banach Spaces and Their Geometry, North-Holland, Amsterdam, 1985.
[5] J.P. Aubin, Applied Functional Analysis, Wiley, New York, 1979.
[6] B.V. Limaye, Functional Analysis, Wiley, New York, 1981.
[7] Z.W. Wang, G.Z. Li, D.R. Guan, X.Y. Yi, Chin. Chem. Lett. 12 (2001) 645.
[8] Z.W. Wang, X.Z. Yi, G.Z. Li, D.R. Guan, A.J. Lou, Chem. Phys. 274 (2001) 57.
[9] Z.W. Wang, G.Z. Li, D.R. Guan, A.J. Lou, J. Colloid Interface Sci. 246 (2002) 302.
[10] M. Schechter, Principles of Functional Analysis, Academic Press, New York, 1971.